Advances in Science and Technology Research Journal

Advances in Science and Technology Research Journal 2024, 18(1), 320–333
https://doi.org/10.12913/22998624/181188
ISSN 2299-8624, License CC-BY 4.0

Received: 2023.12.02
Accepted: 2024.01.05
Published: 2024.01.17

The Influence of the Hot Working Tool Steel Substrate Material on the Element Distribution, Microstructure and Hardness of Gas Metal Arc Welding Hardfaced Layers

Marzena M. Lachowicz[1*], Paweł Sokołowski[1], Marcin Kaszuba[1]

[1] Faculty of Mechanical Engineering, Wrocław University of Science and Technology, Smoluchowskiego 25, 50-372, Wrocław, Poland

* Corresponding author's e-mail: marzena.lachowicz@pwr.edu.pl

ABSTRACT

The paper presents the results of gas metal arc welding (GMAW) hardfacing testing performed on three grades of hot working tool steels, namely: 55NiCrMoV7, X37CrMoV5-1 and modified X38CrMoV5-3 grade. Metallographic investigations, mainly microstructural ones, were carried out and hardness profiles were analyzed. The chemical composition was investigated in each individual layer of the hardfaced deposits and the substrate material, in order to obtain a profile representation. The obtained results of profilometric evaluation of the chemical composition showed clear differences in the content of basic and alloying elements in the subsequent weld layers. The diversity of the chemical composition of the substrate material caused that the uniform chemical composition for all tested materials was achieved only in the third, upper weld layer. Despite the variable content of alloying elements and carbon, as well as slight differences in microstructure occurring for individual weld layers, a substantially stable and high hardness was maintained over the entire cross-section of the obtained hardfaced coatings. In the area of the heat-affected zone (HAZ), a decrease in hardness was observed, which is associated with the decomposition of the high-temperature tempered martensite and the spheroidization of the microstructure.

Keywords: hardfacing, hot work tool steels, die forging, hardness, microstructure, chemical composition, solid solution strengthening, martensite strengthening.

INTRODUCTION

The closed die forging has become widely known as a major player in the forging industry recently. There are many important aspects of this technology that make it a very popular solution in the mass production of small- to medium-sized parts for various industries. The most common advantages include high strength and toughness of produced parts, precision allowing obtaining net or near net shape of elements and limiting post machining, high versatility concerning the shape of components, wide selection of possible feedstock metals and alloys, and many others [1, 2].

However, one of the main limitation of closed die forging is low durability of forming tools, which is a result of demanding working conditions. The analysis of the degradation mechanisms of such tools reveals the effects of a complex interaction of abrasive and/or adhesive wear, oxidation, thermomechanical fatigue, and plastic deformation [3, 4]. In extreme cases, the fatigue cracking of a die was also observed [5]. The deterioration of forming tool brings several serious consequences to the whole forging process. The main issue is the degradation of the quality of forged parts, i.e., occurrence of various forging defects, poor dimensional and shape accuracy of forged parts, etc. [6, 7]. The short tool lifetime has also important economic effects, as the tool itself may account for even 8 to 15% of the total production costs, or even more in case of an unexpected tool's failure [4]. The need to regenerate forging tools results from both economic reasons,

but also with a view to sustainable management of secondary raw materials. Therefore, the possibilities to prevent a tool's failure [8, 9] or to restore die surface [10, 11] were intensively studied over the last years. Below, only the regeneration of forging tools is discussed.

There are several methods of restoring the properties and shape of closed die forging tools prior the complete remanufacture and replacement of a worn tool. The technologically simplest method concerns the so-called re-profiling which means that the upper tool surface is milled down until the free-of-crack, original die cavity is obtained. However, it should be noted that the overall die thickness is simultaneously reduced but also the surface hardness is lowered, as a result of in-depth hardness gradient resulting from usual hardening treatment [12]. For that reason, the rebuilding of forging dies is often considered and welding is the most popular technology in such cases. Countless welding processes are used for that purpose, while the majority of repair welding is done by gas metal arc welding (GMAW) [13, 14] or gas tungsten arc welding (GTAW) [15, 16]. The surfacing processes using high energy density welding processes are being considered recently as well, like plasma transfer arc (PTA) [17, 18] or laser cladding (LS) [19, 20]. The powder-based surfacing processes show quite important advancement in terms of feedstock materials, where the complex composite materials can be applied [21, 22]. The latest studies show also the attempts at using additive manufacturing approaches for local and precise die remanufacturing, mainly by directed energy deposition (DED) processes, like laser metal deposition [23-25] or wire arc additive manufacturing (WAAM) [26]. Finally, quite complex approaches are tested under laboratory- or semi-industrial conditions too, for example, gradient multi-materials wire arc additive remanufacturing presented by Ni et al. [26] or hybrid remanufacturing, where at least two various processes are used, like GMAW hardfacing with further nitriding as described by Kaszuba [27] and Widomski et al. [28]. FCAW-S was also used [29]. Despite the existing literature on the surfacing of these steels, the previous studies did not focus on the aspects of the existing relationship between the chemical composition of the weld metal, microstructure and hardness.

The repair procedure of hot forging tools by hardfacing is a complex task and depends on different factors, among others, it is strongly influenced by the base die material and material to be deposited. The use of welding techniques in the case of tool steels poses significant difficulties due to the high carbon content in these steels. Steels with a carbon content typical of tool steels are difficult to weld. These difficulties result from the increase in carbon content in the weld due to the diffusion of carbon from the additional material into the weld, the possibility of forming structure components with very high hardness, and facilitated overheating in the HAZ. The presence of alloying elements additionally affects these elements. However, thanks to such properties, hardfacing also makes it possible to select additional material to obtain multi-phase layers with wide properties. Ma et al. [30] have shown that, in addition to the chemical composition, the final properties of weld deposits may also be influenced to some extent by the selection of the cooling rate and post-weld heat treatment. Meanwhile, Lange [31] showed that the properties of the obtained welds can be also influenced by flame straightening. Despite significant efforts to develop effective repair methods for hot forging tools, the universal procedures are not widely described in the literature yet.

In this work, the versality of gas metal arc welding method used for hardfacing of three different hot work tool steels is presented. The aim of this work was to study the influence of the base material chemical composition on the microstructure and hardness changes in the successive GMAW weld overlays. As shown earlier, knowledge about the distribution of elements in individual layers in the context of the formed microstructure and its impact on the obtained hardness is a very important issue. From a utilitarian point of view, this work was a first step in developing a robotized process for regeneration of closed die forging tools using the GMAW method.

MATERIALS AND METHODS

Hardfacing process and materials

The real chemical composition of the three hot working tool steels considered in this work is collected in Table 1. The methodology relating to the chemical composition was described in the next section. All steels belong to alloyed chrome-molybdenum steels with the addition of vanadium.

Table 1. Chemical compositions of substrate materials used for hardfacing

Element, wt.%	C	Mn	Si	S	P	Cr	Mo	Ni	V	Fe
1.2714 (55NiCrMoV7, WNLV)	0.60	0.72	0.23	0.005	0.009	0.97	0.43	1.71	0.08	balance
1.2343 (X37CrMoV5-1, WCL)	0.38	0.33	0.86	0.003	0.011	4.80	1.13	0.10	0.33	balance
Modified 1.2367, (mod. X38CrMoV5-3)	0.50	0.45	0.25	-	0.007	5.10	2.21	0.09	0.50	balance

The first two steels tested are standardized grades: 55NiCrMoV7 (1.2714) and X37CrMoV5-1 (1.2343) according to PN-EN ISO 4957:2018-09 standard. The third steel test was non-standardized. The most similar grade in terms of chemical composition is steel X38CrMoV5-3 (1.2367). However, this grade is characterized by a slightly higher value of silicon content and a higher content of molybdenum compared to the tested steel. Vanadium is a highly carbide-forming element. It creates carbides with high hardness and stability at high temperatures. Analogous to molybdenum, it contributes to the effect of secondary hardening. The relatively low carbon content gives these grades quite good ductility and resistance to thermal fatigue.

The hardfacing process was carried out by means of robotized Gas Metal Arc Welding. The GMAW hardfacing was performed by using Lorch SpeedPulse S power source and TOUGH GUN ThruArm robotic gun. The torch was mounted and manipulated by a six-axis robot Yaskawa Motoman HP20. Endotec DO×15 cored wire with a diameter of 1.2 mm was used as a filler material. This is an iron-based feedstock wire with low chromium content. The deposit is characterized by high resistance to cracking and long-term impact, it can be used also at elevated temperatures, up to 600 °C. The mixture of Ar+2.5%CO_2 was used as a shielding gas here. The hardfacing parameters are collected in Table 2, whereas the schematic diagram illustrating the deposition scheme of a three-layer hardfacing deposit is presented in Figure 1. Each substrate material was in a form of a cube with the dimensions of 100×100×50 mm^3.

Initial tests were carried out with various hardfacing parameters. The current (220 and 260A) and gun speed (0.25 and 0.3 m/min) were considered as variables. In this way, four different configurations were obtained, which allowed analyzing the influence of hardfacing linear energy on the microstructure and hardness profiles of deposits. The goal was to achieve a relatively even hardness distribution profile, ensure microstructure homogeneity and hardness gradient without significant changes in the HAZ area. Based on the initial results the final hardfacing parameters were selected (as presented in Table 2) and the further results are presented only for those samples.

Table 2. Hardfacing parameters

GMAW parameter	Hardfacing current, A	Hardfacing voltage, V	Gun speed, m/min	Gas flow rate, slpm
Value	260	30	0.3	17-18

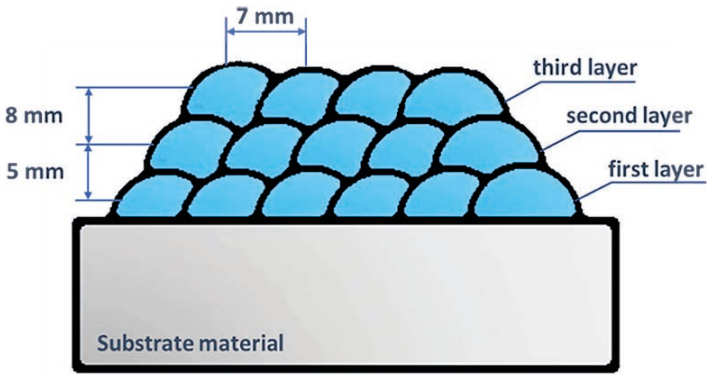

Fig. 1. Schematic diagram of a three-layer hardfacing deposit

Microstructural investigations and hardness measurements

Microscopic examinations were performed on traditionally prepared metallographic samples. For that reason the cross-sections of the obtained weld deposits were prepared. Microstructure assessment was performed using the Leica DM6000M light microscope. The samples were etched using a solution of 3 ml picric acid (99.9%) in ethyl alcohol.

The chemical composition analysis was performed using the Glow-discharge Optical Emission Spectroscopy (GD OES) method on the Leco GDS 500A analyzer. The determined chemical composition of the tested tool materials was summarized in Table 1. In order to obtain a profile analysis, the chemical composition in individual layers of the hardfaced deposits and the base material was analyzed. The specific points were determined on the basis of macroscopic studies. At the same time, the same distance from the hardfaced deposit's surface was maintained, i.e., 5, 10, 13, and 23 mm, respectively. For each of the studied areas, the analysis was carried out twice, and the results are presented as an average value.

Hardness measurements were performed using the Vickers method (Leco AMH55 hardness tester), at a load of 0.5 kgf (HV0.5). The tests were carried out in accordance with the PN-EN ISO 6507-1 standard. Three measurements (called later line A, B and C) were carried out starting from the weld face towards the base material, with a measuring step of about 0.5 mm. Measurements were continued until the hardness values characteristic of the substrate material were noted.

RESULTS AND DISCUSSION

Macroscopic investigations

As part of the preliminary research, macroscopic studies were performed on metallographic macrosamples. These were cross-sections of three-layer hardfaced deposit obtained using the Endotec DO×15 filler (Castolin Eutectic). No welding incompatibilities such as porosity, nonmetallic inclusions or cracks were observed (Fig. 2-4). Individual layers of weld deposit were characterized by high metallurgical purity, good fusion into the base material and between individual layers. The adjacent heat affected zone (HAZ) had a similar thickness, regardless the base material.

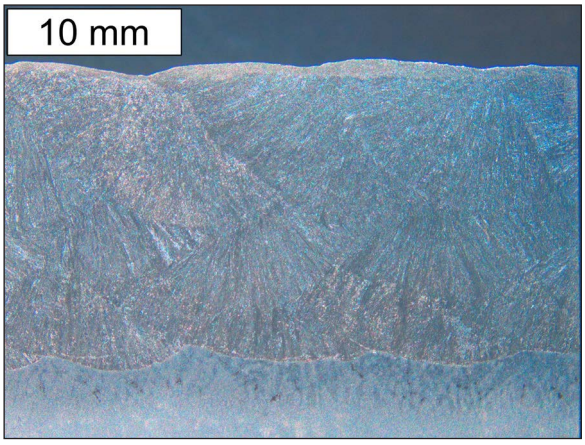

Fig. 2. Macrostructure of the hardfaced deposit obtained using the Endotec DO×15 filler on the 55NiCrMoV7 steel. Etched state, stereoscopic microscopy

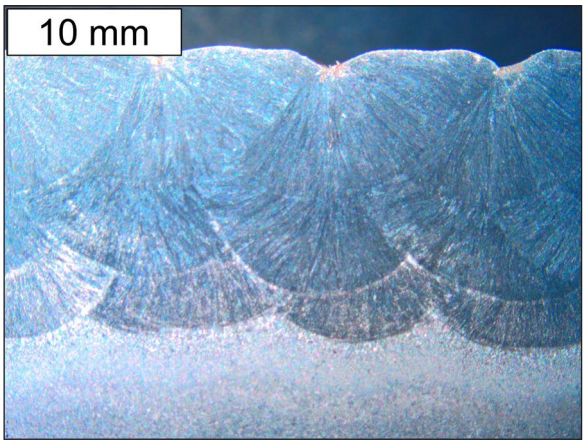

Fig. 3. Macrostructure of the hardfaced deposit obtained using the Endotec DO×15 filler on the X37CrMoV5-1 steel. Etched state, stereoscopic microscopy

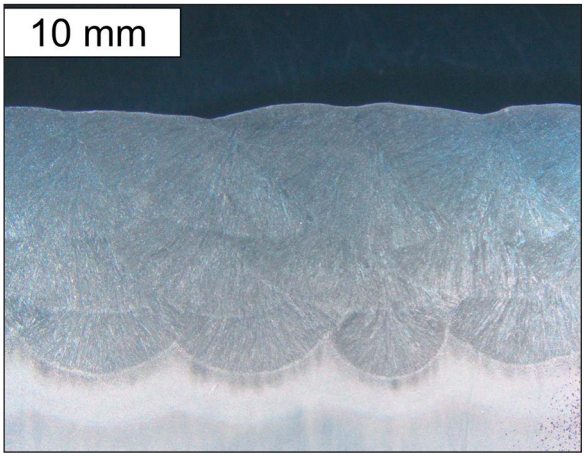

Fig. 4. Macrostructure of the hardfaced deposit obtained using the Endotec DO×15 filler on the modified X38CrMoV5-3 steel. Etched state, stereoscopic microscopy

Microscopic investigations

Microscopic observations were conducted on the prepared metallographic samples, using light microscopy methods in a bright field of view in the characteristic areas of the obtained hardfaced layers. In all the examined deposits, there are columnar grains, perpendicular to the fusion line, with a cellular-dendritic structure. The HAZ was characterized by microstructures depending on the temperature they obtained as a result of heating supplied during hardfacing. The microstructure continuously differed starting from the fusion line until the typical microstructure of the substrate material was reached. The detailed results of microstructural studies are presented below, separately for each grade of base material.

X37CrMoV5-1 steel

In the case of X37CrMoV5-1 hot working steel, the following layers obtained as a result of hardfacing were characterized by heterogeneity in terms of the microstructure. It was observed that the farther away from the surface the area was offset, the more diffusion components were observed in the microstructure. This is due to slower cooling occurring in the layers of the weld located closer to the substrate, as well as reduced carbon content in the area of the first layer, which promotes tempering effect. In the near-surface zone, the dominant component of the microstructure was martensite.

The microstructure in the characteristic areas of the weld deposits is shown in Figure 5. Martensite with the formation of numerous bainite was observed near to the fusion line (Fig. 6a). In the stereoscopic image, bainite was characterized by a lighter color. Areas of dynamic merging of the base material with the filler material were observed on the fusion line. Martensite dominated in the subsequent layers, but locally clusters of bainite were still observed (Fig. 6b, 6c). In the superheat zone occurring in the HAZ directly behind the fusion line, a coarse-grained martensitic or martensitic-bainitic microstructure was observed (Fig. 6d). After the area with a normalized grain size, an area associated with reaching a temperature range close to the A_{C1} line according to in the Fe-Fe_3C diagram appeared. Microstructures indicative of non-equilibrium cooling were observed in that area (Fig. 6e). Directly at the base material, a narrow region was observed where the occurrence of features indicating the presence of heterogeneous decomposition of the tempered martensite and next the resulting spheroidization of the microstructure (Fig. 6f). The first process is similar to the changes occurring during rapid tempering [32]. This resulted in a decrease in hardness which is described later. Finally, a smooth evolution to the microstructure of the base material was observed.

55NiCrMoV7 steel

The microstructure of the examined areas of the hardfaced layers produced on 55NiCrMoV7 steel using DO×15 wire is presented and discussed based on the analyses of characteristic weld zones shown in Figure 7. The area of the weld deposit, as in the case of the previous X37CrMoV5-1 steel, was characterized by a dendritic-cellular microstructure. However, in the case of 55NiCrMoV7 steel, a much more pronounced microstructural homogeneity was observed. The basic microstructural component of the weld deposit was martensite, but numerous lath-like bainite islands occurring in a similar share in all layers were also observed. The fusion line shows continuity between the substrate material and the subsequent layer of the weld deposit (Fig. 8a). Immediately behind it, an area of superheat with a martensite microstructure, heterogeneous in terms of the grain size, was observed. The closer to the substrate material, the more normalized was the grain size in the HAZ area (Fig. 8 e,f). Finally, the microstructure was a fine-grained tempered martensite, smoothly transitioning into the microstructure of the substrate material.

Modified X38CrMoV5-3 steel

In the case of modified X38CrMoV5-3 steel, a very homogeneous microstructure was obtained both in the area of the base material and in the first two layers of the hardfaced zone (Fig. 9, 10). The dominant component of the microstructure in the area of the weld deposit was martensite with single lath-like bainite structures (Fig. 10a, 10b). The cellular-dendritic character of the microstructure was preserved, which was also observed in the case of other tested substrate materials. In the near-surface area of the hardfaced layer, an increased presence of bainite and porosity leading to material discontinuity was observed (Fig. 10c). Above the fusion line, a underheat zone was observed in which coarse-grained martensite was observed, formed from the increased grain of former

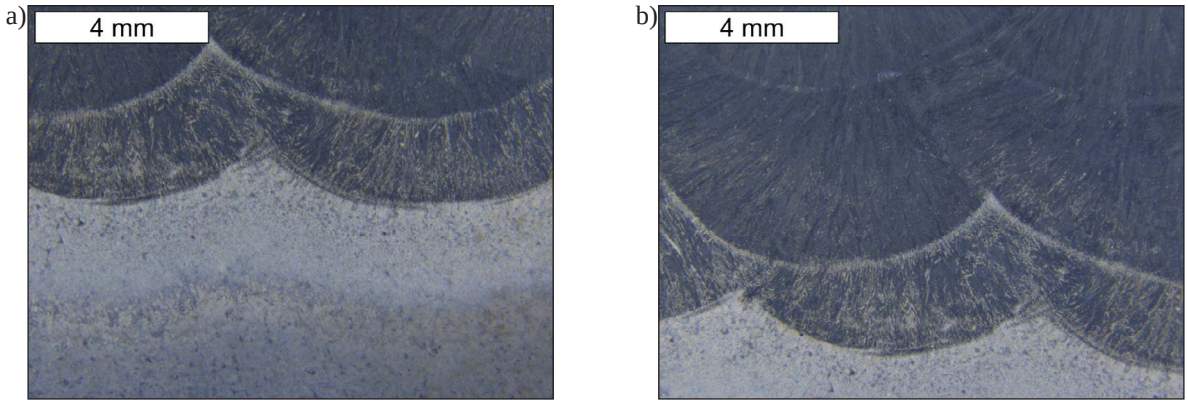

Fig. 5. Stereoscopic image of the area of further microscopic observations for X37CrMoV5-1 base material: a) area from the base material (on the bottom) to the second layer; b) area from HAZ to the third layer of the weld deposit. Stereoscopic microscopy, etched state

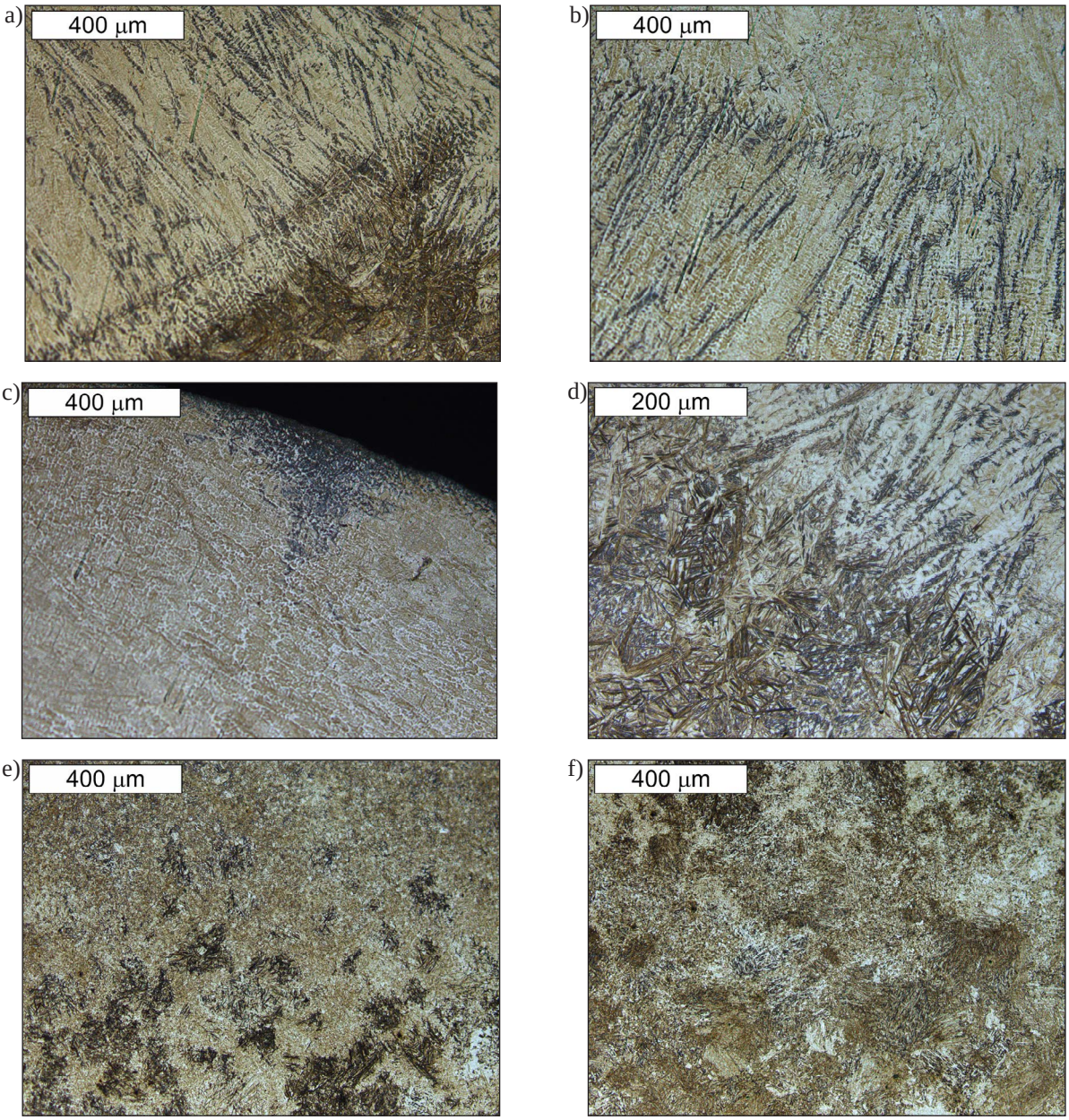

Fig. 6. Microstructure of the hardfaced layers deposited on X37CrMoV5-1 steel grade: a) fusion line, b) transition between the first and second layer, c) third layer, d) fusion line, e, f) heat-affected zone. Light microscopy, etched state

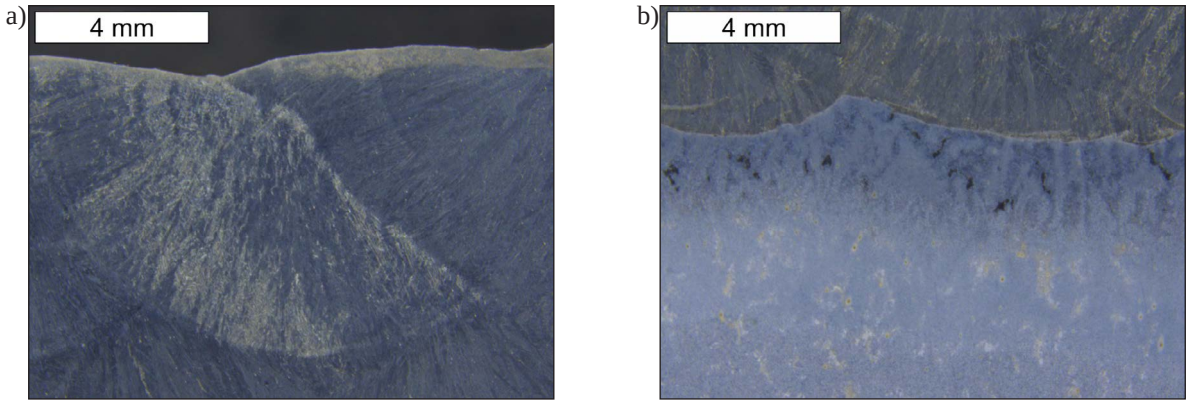

Fig. 7. Stereoscopic image showing the area of microscopic observations for 55NiCrMoV7 base material: a) area of the third and second layer; b) area from HAZ to the first layer of the hardfaced deposit. Stereoscopic microscopy, etched state

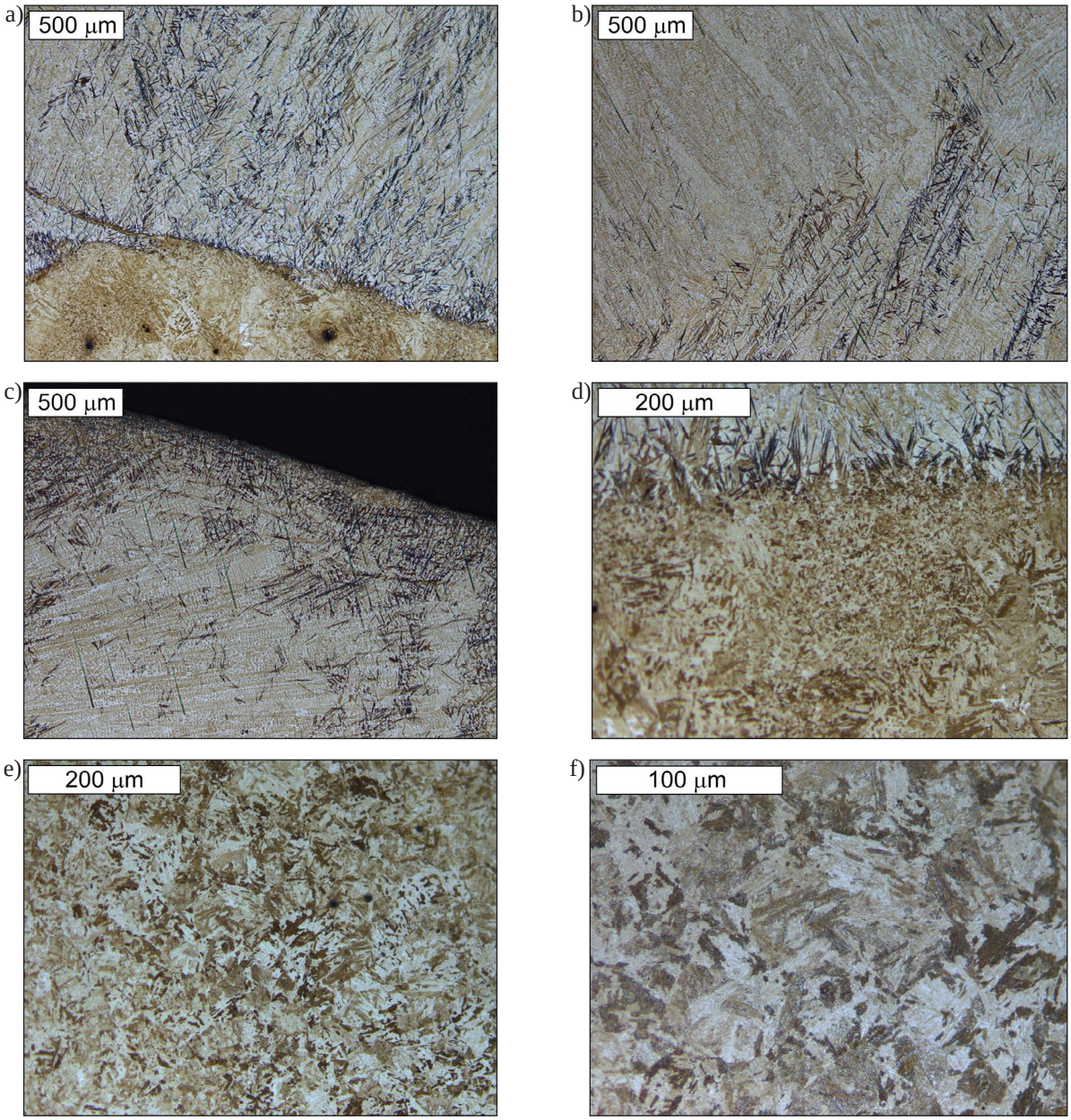

Fig. 8. Microstructure of the weld deposit obtained on the steel grade X37CrMoV5-1: a) fusion line, b) transition between the first and the second layer, c) third layer, d) fusion line, e, f) heat-affected zone. Light microscopy, etched state

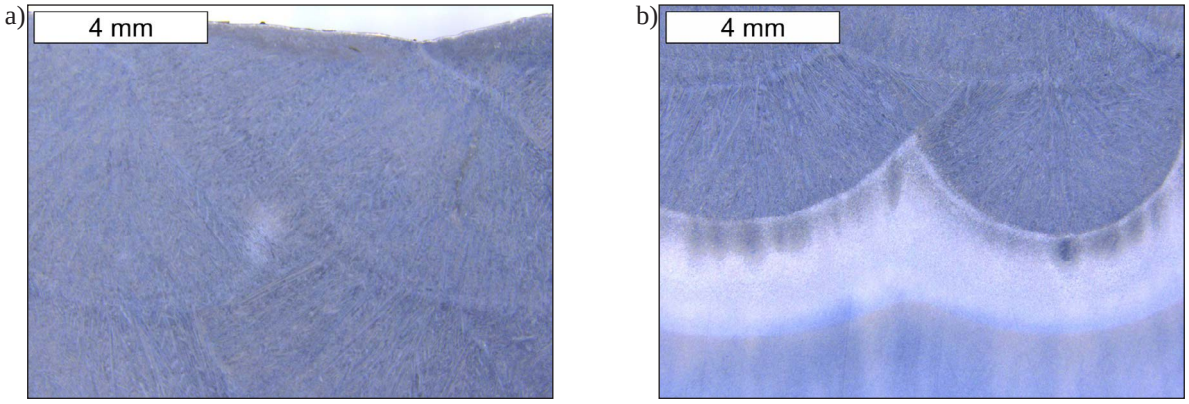

Fig. 9. Stereoscopic image of the area of further microscopic observations for modified X38CrMoV5-3 base material: a) area of the third and second layer; b) area from HAZ to the first layer of the hardfaced layer. Stereoscopic microscopy, etched state

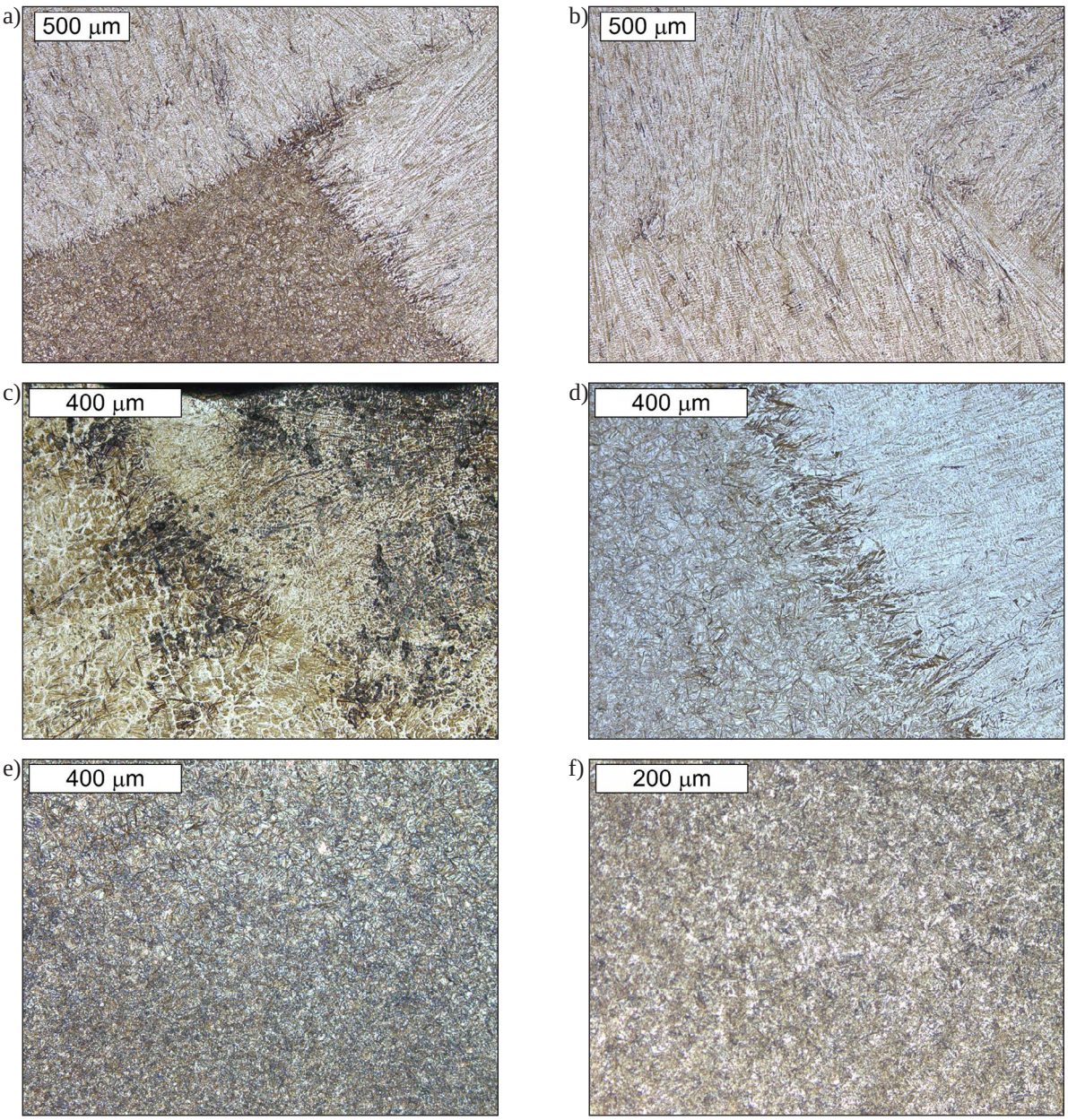

Fig. 10. Microstructure of the weld deposit obtained on modified X38CrMoV5-3 steel: a) fusion line, b) transition between the first and the second layer, c) third layer, d) fusion line, e, f) heat-affected zone. Light microscopy, etched state

austenite. It was accompanied by an increased content of residual austenite. Behind it, there was a zone of fine-grained martensite smoothly passing into the base material (Fig. 10d-f).

Chemical composition analysis

The properties of the hardfaced layers are strongly dependent on the distribution of basic and alloying elements. In order to determine the degree of merging of base material and weld deposit, an analysis of the chemical composition was carried out along the hardfacing cross-section. Figures 11 and 12 show changes in concentration determined for basic elements (C, Mn, Si), as well as alloyed elements. The analyses were presented in the direction from the surface to the base material. The analyses omitted the contents of sulfur and phosphorus due to their low content in tested materials.

The analysis showed large differences in the content of elements in the tested samples (Fig. 11). Substrate materials as a result of convective movement in the liquid pool of the area of the forming weld deposit are intensively mixed with the hardfacing feedstock material. The highest degree of merging was observed for the first layer located just above the fusion line. The content of basic and alloying elements in the first layer of the weld significantly depends on the substrate material, which also causes heterogeneity of the chemical composition of the weld deposit. The change in the concentration of the elements of the base material in the weld deposit decreases obviously in the second and third layer. In the case of carbon, its lower content in X37CrMoV5-1 and modified X38CrMoV5-3 steels in relation to the hardfacing wire resulted in its lower content in the first layer of the weld deposit compared to the subsequent layers. In the case of 55NiCrMoV7 steel, the opposite trend was observed, i.e., a higher carbon content in the area of the first layer of the weld deposit was noticed. A similar relationship was observed for silicon, which higher concentration in X37CrMoV5-1 steel translated into an increase in the silicon content in the first layer of the weld deposit in relation to the subsequent layers. Meanwhile, a decrease in silicon in similar hardfaced layer region was recorded for the other two steel substrates, i.e., the concentration of silicon increased in the upper weld deposit layers, to reach a constant value in the third layer. Noteworthy, however, is the more pronounced decrease in silicon in the first layer in the case of modified X38CrMoV5-3 steel compared to 55NiCrMoV7 steel, despite the fact that both are characterized by a similar silicon content in as-produced state. In the third layer, no differences in the chemical composition of the hardfaced layers obtained on tested base steels were found, which indicates that this area is already devoid of the influence of initial chemical composition of the substrate. Directly at the surface, and therefore in the third layer, a constant chemical composition

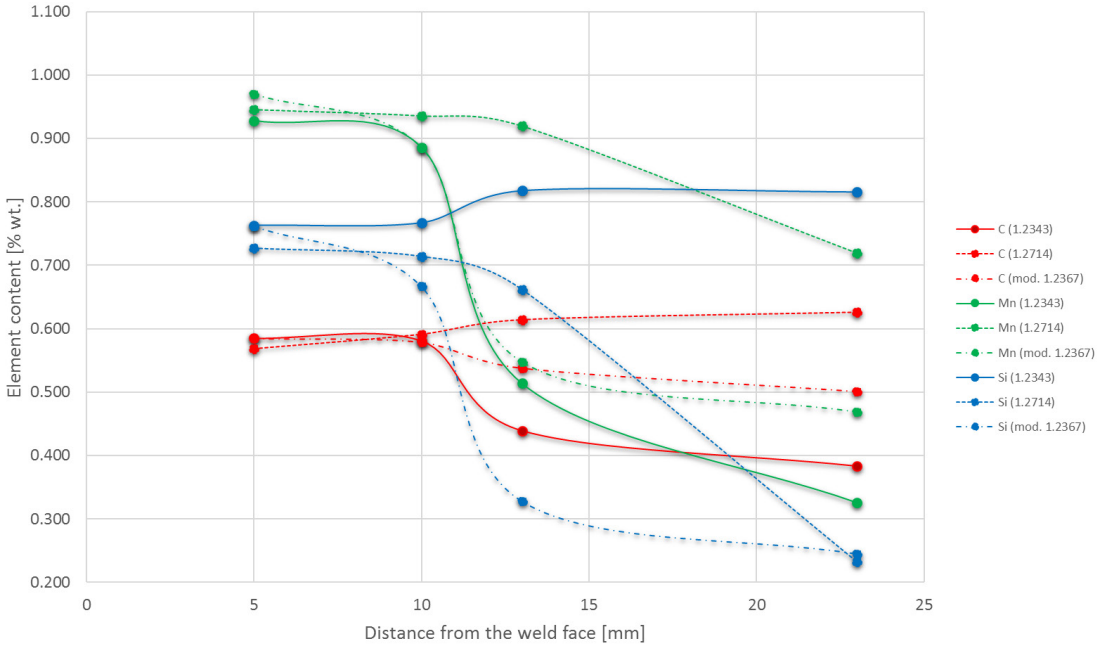

Fig. 11. Change in the content of basic elements in the tested weld deposits

was observed regardless of the substrate material. This applies to both, basic elements with a negligible content and alloying elements occurring in higher concentrations.

In case of alloying elements, a significant decrease in chromium in the first layer of the hardfaced layers of all tested materials was clearly visible (Fig. 12). This element is involved in the formation of carbides, the presence of which affects the hardness of the obtained weld deposits. The most pronounced decrease in chromium content was observed in the case of 55NiCrMoV7 steel, which is characterized by a low content of this element. Significant differences in the content of chromium between the hardfacing wire and the base material resulted in a decrease in its content in the first two layers of the obtained layers. Chromium also promotes the tempering of steel. In this respect, the decrease in chromium content in the welds made on 55NiCrMoV7 steel should be compensated by an increasing carbon content. In the case of X37CrMoV5-1 and modified X38CrMoV5-3 steels, the chromium concentration was stabilized already in the second layer. In the case of modified X38CrMoV5-3 steel, an increase in the molybdenum content in the first layer, which is an element forming stable carbides, was observed. This is due to the higher Mn content in this base material and this should favor higher hardness in this area. The third layer of all investigated hardfaced layers had a higher tungsten content compared to the base materials tested, which was affected by an increased tungsten content in the hardfacing wire. On the other hand, the low content of nickel in the feedstock wire caused a gradual decrease in this element, starting from the substrate up to the third layer. This was especially visible in case of 55NiCrMoV7 steel, which contains highest Ni content among the tested hot working steel substrates. Finally, vanadium showed similar content along the whole measurement line, in all analyzed cases.

Hardness profiles

Hardness measurements were made using the Vickers method. The test was carried out along three lines, each time the measurements starting directly at the surface and ending in the base material, outside the heat-affected zone. In the case of two lines, the measurements were made by making imprints at a fine step, but over a length of 20 mm. For the third line, fewer hardness measurements were made, but over a longer distance to confirm the hardness stability outside the weld area.

The hardness obtained in the weld deposit, in particular in the first layer, is the result of structures caused by the merging of substrate materials with the hardfacing wire. In the case of X37CrMoV5-1 steel, the lower content of carbon and alloying elements of the first layer in relation to the last layer did not significantly affect

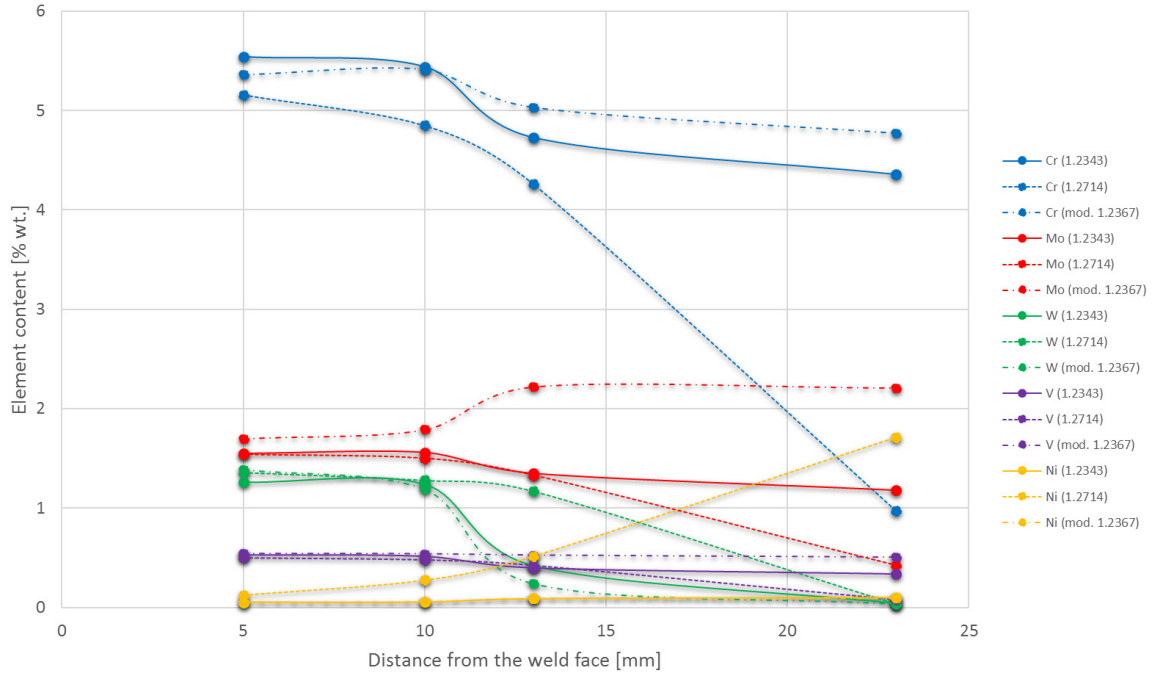

Fig. 12. Change in the content of alloying elements of the tested weld deposits

the hardness in the hardfaced layer. Tests carried out on the cross-section of the layer deposited on X37CrMoV5-1 steel showed rather stable hardness profile of around 700 HV0.5, locally exceeding 800 HV0.5. This means that phase strengthening is dominant in this area, resulting from the presence of martensitic and bainitic structures. The obtained results were characterized by a certain instability of hardness directly behind the fusion line, which should be combined with the presence of martensitic or martensitic-bainitic microstructures with differentiated grain in this region. The transition to the base material was followed by a decrease in hardness near the place where the material reached a temperature close to A1 and the resulting spheroidization of the microstructure (Fig. 13).

Analyzing the results for 55NiCrMoV7 steel, it can be concluded that the hardness in the hardfaced layer locally increased nearly up to 900 HV0.5 (Fig. 14). Therefore, it was possible to obtain higher hardness compared to X37CrMoV5-1 steel, despite the greater share of bainitic structures in the weld deposit area. This is related to the higher carbon content in the base material, which allowed to obtain higher carbon content

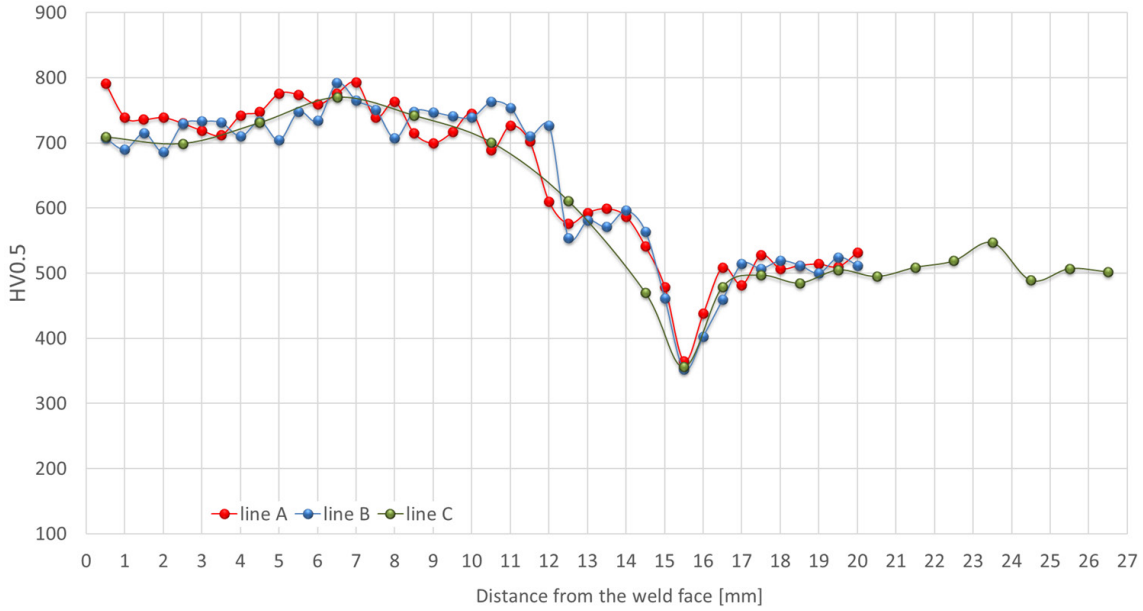

Fig. 13. Hardness distribution for the hardfaced layers obtained on X37CrMoV5-1 steel

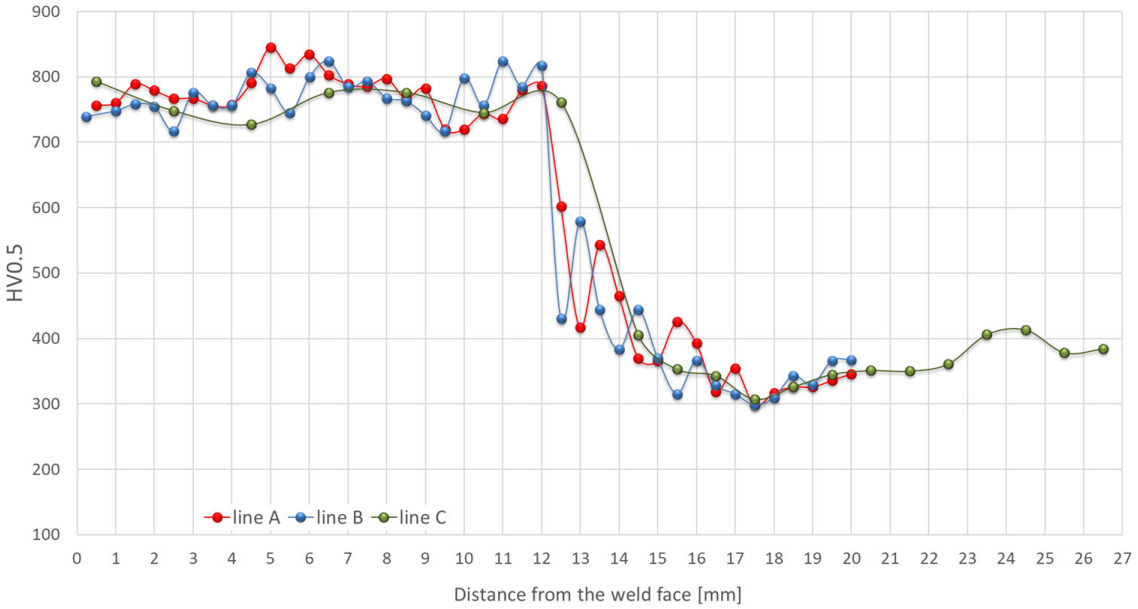

Fig. 14. Hardness distribution for the hardfaced layers obtained on 55NiCrMoV7 steel

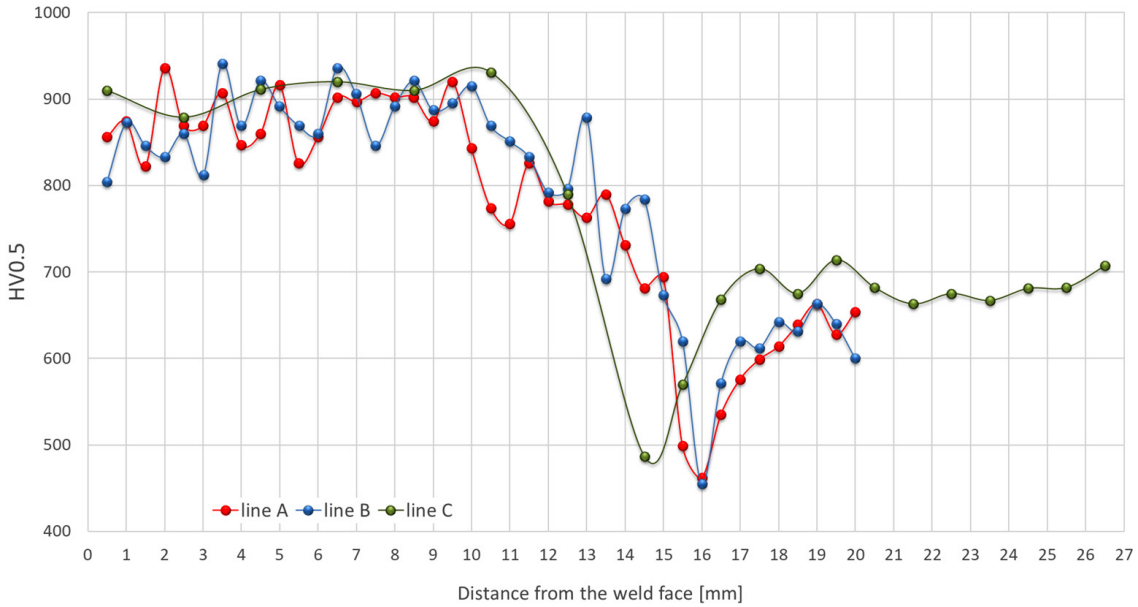

Fig. 15. Hardness distribution for the hardfaced layers obtained on modified X38CrMoV5-3 steel

in the first layer of the weld, and thus a greater degree of carbon saturation of the forming martensite and bainite. The transition of the weld to the base material was accompanied by a decrease in hardness to the value characteristic of the base material. No decrease in hardness was observed below typical values for the 55NiCrMoV7 steel, which was the case of X37CrMoV5-1 steel. However, this should be associated primarily with the lower hardness of the substrate material itself, i.e., 55NiCrMoV7 steel, compared to other investigated substrates.

In the case of modified X38CrMoV5-3 steel, the high content of alloying elements was accompanied by the highest hardness of the obtained layers (Fig. 15). This is associated with the formation of simple carbides, as well as the reinforcement of the matrix solution. Similarly as in the case of X37CrMoV5-1 steel, a decrease in hardness associated with the decomposition of the tempered martensite and coagulation of carbide precipitates was observed in the HAZ area. Noteworthy is the higher hardness observed in this zone, related to the tempering of the base material. This steel has the highest content of molybdenum and vanadium, which create very stable carbides and high hardness. For this reason, despite the tempering taking place, the hardness remains at a much higher level than in the case of other steels. However, the obtained results were characterized by quite significant instability, in particular behind the fusion line. It is associated with an increased amount of residual austenite occurring in this area. The transition of the hardfaced layer to the base material was accompanied by a decrease in hardness to the value characteristic of the base material, as in the case of X37CrMoV5-1 steel.

CONCLUSIONS

In this work the GMAW hardfacing process was carried out using three different hot working tool steels (55NiCrMoV7, X37CrMoV5-1 and modified X38CrMoV5-3). Based on the conducted microstructural studies, chemical composition analysis and hardness measurements, the following conclusions can be drawn:

1. The obtained results of profilometric tests of the chemical composition showed clear differences in the content of basic and alloying elements in the weld deposits. The content of alloying elements in the first layer of the layer significantly depended on the substrate material, leading to heterogeneity of the chemical composition of the hardfaced deposit. The change in the concentration of the components of the base material diffused in the weld decreased in the upper layers of deposits. In the third layer, directly at the surface, a uniform chemical composition of the deposit independent of the substrate material was observed. This conclusion has great utilitarian significance because it indicates the number of layers that are required to obtain properties typical of the additional material used.

2. The microstructure of the weld deposits was characterized mainly by a martensitic microstructure with a variable share of residual austenite and locally occurring bainite. The present differences were the main reason for the slight differences in the hardness of individual, investigated hardfaced layers. The microstructure of the tested substrate materials was tempered martensite.
3. In the area of the obtained weld deposits, despite the variable content of alloying elements and carbon, as well as slight differences in hardness occurring for individual layers, a substantially stable hardness was obtained over the entire cross-section. This indicates that phase transformation strengthening is dominant in this area, resulting from the presence of martensitic and bainitic structures. Tests carried out on the cross-section of the layer deposited on X37CrMoV5-1 steel showed rather stable hardness profile of around 700 HV 0.5, locally exceeding 800 HV 0.5. Analyzing the results for 55NiCrMoV7 steel, it can be concluded that the hardness in the hardfaced layer locally increased to almost 900 HV0.5. Similar values were also obtained for modified X38CrMoV5-3 steel.
4. The heat-affected zones showed microstructures depending on the temperature they obtained during hardfacing in the analyzed cases. These microstructures changed starting from the transition line until they reached an intact microstructure of the substrate material. In each case, in the HAZ region, a decrease in hardness was observed. This is the region in which the material heated during hardfacing process reached a temperature close to A_1 according to the Fe-Fe_3C chart. The decrease in hardness was associated with the high-temperature decomposition of the tempered martensite and the spheroidization of the microstructure. Then, the hardness smoothly reached the values characteristic of the base materials.

REFERENCES

1. Jaiswal T., Ingle V.A Review on closed die forging. International Journal of Advances in Engineering and Management 2022; 4(7): 601-605.
2. Tomov B. Hot closed die forging – State-of-Art and future development. Journal of Achievement in Materials and Manufacturing Engineering 2007; 24(1): 443-449.
3. Rajiev R., Sadagopan R., Shanmuga Prakash R. Study on investigation of hot forging die wear analysis – An industrial case study. Materials Today: Proceedings 2020; 27(3): 2752–2757.
4. Gronostajski Z., Kaszuba M., Hawryluk M., Zwierzchowski M. A review of the degradation mechanisms of the hot forging tools. Archives of Civil and Mechanical Engineering 2014; 14(4): 528–539.
5. Hawryluk M., Lachowicz M., Łukaszek-Sołek A., Lisiecki Ł., Ficak G., Cygan P. Structural Features of Fatigue Crack Propagation of a Forging Die Made of Chromium–Molybdenum–Vanadium Tool Steel on Its Durability. Materials 2023; 16: 4223.
6. Hawryluk M., Kondracki P., Krawczyk J., Rychlik M., Ziemba J. Analysis of the impact of forging and trimming tools wear on the dimension-shape precision of forgings obtained in the process of manufacturing components for the automotive industry. Eksploatacja I Niezawodność – Maintance and Reliability 2019; 21(3): 476–484.
7. Krajewska-Spiewak J., Turek J., Gawlik J. Maintenance Supervision of the Dies Condition and Technological Quality of Forged Products in Industrial Conditions. Management and Production Engineering Review 2021; 12(2): 27-32.
8. Emamverdian A.A., Sun Y., Cao C., Pruncu C., Wang Y. Current failure mechanisms and treatment methods of hot forging tools (dies) - a review. Engineering Failure Analysis 2021; 129: 105678.
9. Gronostajski Z., Hawryluk M., Widomski P., Kaszuba M., Nowak B., Polak S., Rychlik M., Ziemba J., Zwierzchowski M. Selected effective methods of increasing the durability of forging tools in hot forging processes. Procedia Manufacturing 2019; 27: 124-129.
10. Chen C., Wang Y., Ou H., He Y., Tang X. A review on remanufacture of dies and moulds. Journal of Cleaner Production 2014; 64: 13–23.
11. Bin C. Repairability Evaluation of Retired Hot Forging Die Based on Matter-Element Extension Model. Journal of Physics: Conference Series 1986, 1: 012131.
12. Kopas P., Sága M., Nový F., Paulec M. Influence of re-profiling on the premature failure of hot forging dies. Engineering Failure Analysis 2023; 152: 107507.
13. Zhang M., He S., Jiang B., Yao X., Zhang K. The Study on Feasibility and Welding Characteristics of GMAW Surfacing Remanufacturing of H13 Steel Cutter Ring of TBM Hob. Coatings 2021; 11(12): 1559.
14. Widomski P., Kaszuba M., Krawczyk J., Nowak B., Lange A., Sokołowski P., Gronostajski Z. Investigating the Possibility of Regenearation by Hardfacing for Forging Tools Based on Analysis

of Tool Working Conditions and Wear Evaluation. Archives of Metallurgy and Materials 2022; 67(4): 1395–1410.

15. Kashani H., Amadeh A., Ghasemi H.M. Room and high temperature wear behaviors of nickel and cobalt base weld overlay coatings on hot forging dies. Wear 2007; 262(7): 800–806.
16. Pelcastre L., Kurnia E., Hardell J., Decrozant-Triquenaux J., Prakash B. High temperature tribological studies on hardfaced tool steels for press hardening of Al-Si coated boron steel. Wea 2021; 476: 203728.
17. Jhavar S., Paul C.P., Jain N.K. Micro-Plasma Transferred Arc Additive Manufacturing for Die and Mold Surface Remanufacturing. JOM 2016; 68(7): 1801–1809.
18. Wang H., Liu Q., Han N., Yao L., Zhu C. Three-Point Bending Fracture Properties of Multilayer Metal Hot Forging Die Specimen. IOP Conference Series: Materials Science and Engineering 2019; 472(1): 012033.
19. Yin Y., Wang Y., Tan Z.R., Yu W.J. Cr12MoV Die Repair Experiment Based on Laser Cladding with Wire. Key Engineering Materials 2019; 814: 137–143.
20. Kattire P., Paul S., Singh R., Yan W. Experimental characterization of laser cladding of CPM 9V on H13 tool steel for die repair applications. Journal of Manufacturing Processes 2015; 20(3): 492–499.
21. Appiah A.N.S., Bialas O., Żuk M., Czupryński A., Sasu D.K., Adamiak M. Hardfacing of Mild Steel with Wear-Resistant Ni-Based Powders Containing Tungsten Carbide Particles Using Powder Plasma Transferred Arc Welding Technology. Materials Science-Poland 2022; 40(3): 42–63.
22. Poloczek T., Lont A., Górka J. Structure and Properties of Laser-Cladded Inconel 625-Based in Situ Composite Coatings on S355JR Substrate Modified with Ti and C Powders. Materials Science-Poland 2022; 40(4): 14–27.
23. Devine R., Cullen C., Foster J., Kulakov M., MacFadden C., Fitzpatrick S. Remanufacture of Hot Forging Dies By LMD-p Using a Cobalt Based Hard-Facing Alloy. BHM Berg- und Hüttenmännische Monatshefte, 2021; 166: 243–249.
24. Foster J., Cullen C., Fitzpatrick S., Payne G., Hall L., Marashi J. Remanufacture of hot forging tools and dies using laser metal deposition with powder and a hard-facing alloy Stellite 21®. Journal of Remanufacturing 2019; 9(3): 189–203.
25. Asnafi N. Tool and Die Making, Surface Treatment, and Repair by Laser-based Additive Processes. BHM Berg- und Hüttenmännische Monatshefte 2021; 166(5): 225–236.
26. Ni M., Hu Z., Qin X., Xiong X., Ji F. Microstructure and Mechanical Properties of Gradient Interfaces in Wire Arc Additive Remanufacturing of Hot Forging Die Steel. Material 2023; 16(7): 2639.
27. Kaszuba M. The application of a new, innovative, hybrid technology combining hardfacing and nitriding to increase the durability of forging tools. Archives of Civil and Mechanical Engineering 2020; 20(4): 122.
28. Widomski P., Kaszuba M., Sokołowski P., Lange A., Walczak M., Długozima M., Gierek M., Chocyk D., Gładyszewski G., Boryczko B. Nitriding of Hardfaced Layers as a Method of Improving Wear Resistance of Hot Forging Tools. Archives of Civil and Mechanical Engineering 2023; 23(4): 241.
29. Kaszuba M., Widomski P., Białucki P., Lange A., Boryczko B., Walczak M. Properties of new-generation hybrid layers combining hardfacing and nitriding dedicated to improvement in forging tools' durability. Archives of Civil and Mechanical Engineering 2020; 20: 78.
30. Ma C., Wu Z., Qi Y., Zhang X.. Effect of heat treatment and cooling rate on microstructure and properties of T92 welded joint. Materials Science-Poland. 2023; 41(1): 124-139.
31. Lange, A. Influence of flame straightening on the properties of welded joints made of X2CrNi22-2 duplex steel. Materials Science-Poland 2021; 39, 446–457.
32. Królicka, A.; Żak, A.; Kuziak, R.; Radwański, K.; Ambroziak, A. Decomposition mechanisms of continuously cooled bainitic rail in the critical heat-affected zone of a flash-butt welded joints. Materials Science-Poland. 2021, 39, 615–625.